Available online at www.sciencedirect.com
SCIENCE DIRECT
Polymer 46 (2005) 3481–3488
polymer
www.elsevier.com/locate/polymer

Molecular dynamics simulation of PAMAM dendrimer in aqueous solution

Ming Han[a,*], Peiquan Chen[b], Xiaozhen Yang[a]

[a]State Key Laboratory of Polymer Physics and Chemistry, Institute of Chemistry, Chinese Academy of Sciences, Beijing 100080, China
[b]Department of Chemistry, Nankai University, Tianjin 300071, China

Received 11 November 2004; received in revised form 12 February 2005; accepted 12 February 2005
Available online 26 March 2005

Abstract

The properties of ethylenediamine (EDA) cored and amine surface poly(amidoamine) (PAMAM) dendrimers of generation 1 through 7 in the explicit solvent were studied by the atomistic force field based molecular dynamics. Since amines are assumed to be protonated the simulation condition is designed to represent the dilute alkali solution. All the generations are spherical in shape, while the higher generations show edges or slightly polyhedral shape. The density profile indicates that the dendrimers are constant density spheres and the densities are independent of generation in this aqueous solution. The scaling properties of the radius of gyration with the numbers of atoms and solvent accessible surface with radius of gyration indicate the PAMAM dendrimers are densely compact structures which result from the highly flexibility confirmed by the terminal group distribution. Dynamic behaviors such as autocorrelation function of the squared radius of gyration and mean square displacement were also studied too.

Keywords: Molecular dynamics; PAMAM dendrimer; Dendrimer solution

1. Introduction

Dendritic molecules possess three distinguishing architectural components: an initiator core; interior layers often called 'generations' which comprise repeating units radially attached to the initiator core and exterior (terminal functionality) attached to the outermost interior generation. The well defined, highly branched, compartmentalized structures in the nanometer size range exhibit unique properties such as high degree of molecular uniformity, narrow molecular weight distribution, specific size and shape characteristics, a highly-functionalized terminal surface. Dendrimers have become a subject of soft-matter physics within the last few years. The analytical theory of dendritic structures has progressed considerably and a great number of simulations are now available [1].

Tomalia et al. first reported the synthesis of PAMAM dendrimers in the early 1980s [2]. PAMAM dendrimers have become one kind of the most widely used dendrimers and are commercially available now. Their applications range from drug delivery to molecular encapsulation and gene therapy, from building blocks for nanostructures to micelle mimics as decontaminating agents [3,4].

Maiti and Goddard et al. [5] characterized the properties for generations up to the limiting growth size by atomistic based molecular dynamics only in the gas phase. Lee et al. [6] carried out molecular dynamics simulations of PAMAM dendrimers of generation 2 through 6 at several pH values by introduction of a simple dielectric constant to try to simulate the aqueous solution systems without explicit water. The simplified method does not provide an accurate description of the physics of the systems because solvents have a major effect on the structure and properties of dendrimers. It is necessary to employ realistic models to simulate the solvent molecules, so we include the explicit solvent water in this present MD simulation. The static properties of the PAMAM dendrimers in aqueous solution such as particle size, shape information, monomer density distribution, terminal amine group distribution, solvent accessible surface and dynamic properties such as autocorrelation function of the squared radius of gyration, mean

* Corresponding author. Tel.: +86 10 8261 8423; fax: +86 10 6257 1123.
E-mail address: hanming@iccas.ac.cn (M. Han).

0032-3861/$ - see front matter © 2005 Elsevier Ltd. All rights reserved.
doi:10.1016/j.polymer.2005.02.107

square displacement were discussed in this paper. As to our knowledge this is the first work to simulation the dendrimers with the real chemical units as high as generation 7 in the explicit water.

2. Method

The initial ethylenediamine (EDA) cored and amine surface poly(amidoamine) (PAMAM) models were built in the Material Studio software package of Accelerys Inc. The molecular weight, atom number and surface group number are listed in Table 1 for generation 1 through 7. The charges on the dendrimer are derived from ab initio calculation of the repeating units by Gaussian '03 software.

The solvation and molecular dynamics simulations were run using GROMACS package v3.2.1 [7,8] which is primarily designed for biochemical molecules. PAMAM is a kind of peptide dendrimers so GROMACS force field fits this system. Atomic detail is used except for hydrogen atoms bound to carbon atoms, which we treated as united atoms and no special hydrogen-bond term is included. The water is modeled according to the single point charge (SPC) model [9]. The rhombic dodecahedron is used as the box type for periodic boundary conditions whose volume is 0.71 of that of a cubic box with the same periodic image distance. The length of the box vector is long enough to exceed the length of the macromolecule in the direction of that edge plus two times the cutoff radius. The number of water molecules in the simulated system and the size of the box are listed in Table 1. The density of the systems is about 980 (kg/m^3). A group based twin cutoff scheme was employed for the nonbonded interactions, with $R_{cut}=0.8$ nm for Lennard–Jones and $R_{cut}=1.4$ nm for electrostatic interactions. The system was coupled to an isotropic pressure bath of 1 atm. via a coupling constant of $\Gamma_p=1.0$ ps and a ear bath of 300 K using standard coupling schemes [10] with a coupling constant of $\Gamma_t=0.1$ ps. Using the fast LINCS [11] and SETTLE [12] algorithms to constrain the bond lengths within the dendrimers and to constrain the water geometry respectively. These simulations had a time step of 3 fs, the length of the simulations is listed in Table 1 too.

MD simulations were performed on a PC cluster with 24 nodes. Other analyses used GROMACS or locally written code. We employ MD simulations to anneal the structures and then to collect the equilibrium data to extract the properties of these dendrimers.

3. Result and discussion

In different pH solution and salt concentration the properties and size of the dendrimers change a lot. In this paper no amines are assumed to be protonated. This simulation condition is designed to represent the effect above pH 10 based on pH titration data [6].

3.1. Equilibration

The equilibration of the systems was monitored through the potential energy and the radius of gyration. The energy and radius of gyration of all the generations stabilized within the first 1500 ps. The measure of the relaxation of dendrimer molecules is determined from the autocorrelation function of the squared radius of gyration, $C_{R_g}(t)$, which is evaluated from the expression:

$$C_{R_g}(t)=\frac{\langle(R_g^2(t)-\langle R_g^2\rangle)(R_g^2(0)-\langle R_g^2\rangle)\rangle}{\langle R_g^4\rangle-\langle R_g^2\rangle^2}$$

The relaxation times t_{R_g} for the seven generations, where $C_{R_g}(t_{R_g})=1/e$, obtained from Fig. 1 are listed in Table 1. According to the relaxation times the simulation times are long enough to sample to give enough independent configurations for sufficient averaging of the static properties. We did not find the apparent dependence of the relaxation time on the generation numbers.

3.2. Dendrimer size and shape

3.2.1. Radius of gyration

Radius of gyration is especially useful to characterize polymer solutions to have a rough measure for the compactness of a structure. It is calculated as follows:

$$R_g=\left(\frac{\sum_i ||r_i||^2 m_i}{\sum_i m_i}\right)^{\frac{1}{2}}$$

Table 1
Properties of PAMAM by generation and simulation details

Generation	Surface group number	Molecular weight	Atom number	Box vector [nm]	Water number	Length of the simulations [ps]	Relaxation times, t_{R_g}, [ps]
1	8	1429.88	228	3.93	1203	15,000	419
2	16	3256.4	516	5.12	2965	15,000	352
3	32	6908.98	1092	6.57	6257	15,000	412
4	64	14214.5	2244	7.04	7322	15,000	373
5	128	28825.4	4548	8.10	10916	9900	322
6	256	58047.3	9156	10.72	25804	7400	312
7	512	116491	18372	11.89	33242	4500	317

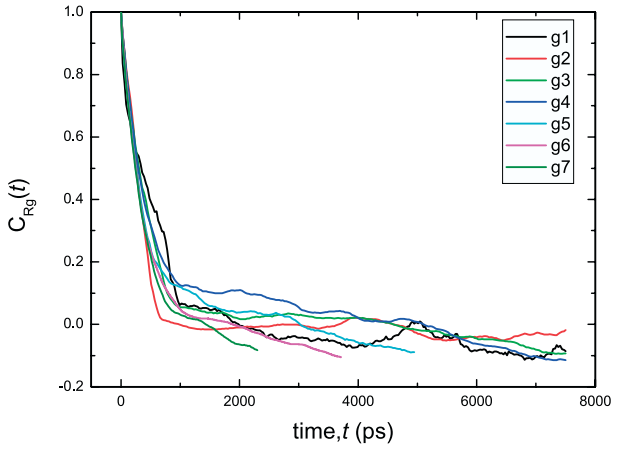

Fig. 1. Autocorrelation function of the squared radius of gyration.

where m_i is the mass of atom i and r_i the position of atom i with respect to the center of mass of the molecule.

Fig. 2a shows the radius of gyration as a function of generation. We compare the radius of gyration from this simulation with the data from small angle X-ray scattering (SAXS) experiment on dilute methanol solutions [13]. Our data are less than the data obtained form the SAXS experiment. This discrepancy results from the difference in conditions. The electrostatic repulsive interaction from the protonation of the nitrogen atoms in the solutions will make the dendrimers swell. In the future we should perform the simulation about the protonized state of the dendrimers, where the electrostatic interaction will be considered more carefully. However, the simulation time will increase largely. Fig. 2b shows the relationship between the number of atoms in PAMAM and the radius of gyration of PAMAM on a double-logarithmic scale. The number of atoms scales as $N \sim R_g^{2.93}$. The calculated exponent 2.93 is almost 3, indicating that these PAMAM dendrimers have a homogeneous structure in which the atoms are densely packed. The scaling exponent agrees well with the Brownian dynamics simulation by Murat and Grest [14] and SAXS experiment [13]. This compact structure requires a space filling geometry that implies considerable back-folding of the outer generations.

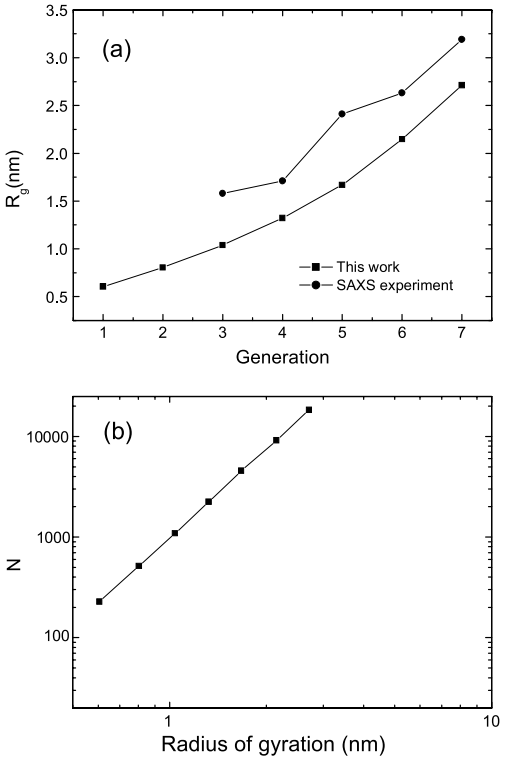

Fig. 2. (a) Radius of gyration of the PAMAM as a function of the generation number. (b) Relationship between the number of atoms in PAMAM and the radius of gyration of PAMAM on a double-logarithmic scale.

3.2.2. Asphericity

Typical equilibrated conformations of the seven dendrimer generations are shown in Fig. 3. The hydrogen atoms are depicted white, carbon atoms cyan, nitrogen atoms blue and oxygen atoms red. These snapshots are generated using VMD software [15] developed at UIUC. In the condition we simulate all the generations are spherical in shape although they are not so perfect. Higher generation dendrimers show edges or slightly polyhedral shape, which agrees with the TEM images in the real experiments [16]. In order to provide quantitative criteria the geometry of the simulated dendrimers is examined by the moment of inertia. The average values of the three principal moments of inertia I_z, I_y, I_x, where I_z, I_y, I_x represent the eigenvalues of the moment of inertia tensor in descending order, are tabulated in Table 2. Fig. 4a shows the average aspect ratios I_z/I_x and I_z/I_y for different generation dendrimers. The values of I_z/I_y are in the range 1.1–1.3 and I_z/I_x are in the range 1.3–1.5. This means that these dendrimers are compact spheres in shape. The change in shape is reflected on the relative shape anisotropy, which is defined as [17]:

$$\kappa^2 = 1 - \frac{3\langle I_2 \rangle}{\langle I_1^2 \rangle}$$

where I_1 and I_2 are the first and second invariants of the radius of gyration tensor: $I_1 = I_x + I_y + I_z$, $I_2 = I_x I_y + I_y I_z + I_x I_z$. This quantity assumes values between 1 (for a linear array of atoms) and 0 (for shapes of high 3-d symmetry). In Fig. 4b the relative shape anisotropy of simulated dendrimers are near zero so it also reveals strongly compact

Table 2
Three principal moments of inertia I_x, I_y, I_z

Generation	I_x [a.m.u. nm^2]	I_y [a.m.u. nm^2]	I_z [a.m.u. nm^2]
1	270.6	348.5	401.1
2	1096.5	1424.1	1592.4
3	4051.7	5062.7	5498.4
4	13213.9	17147.3	18333.9
5	45871.6	54071.5	57584.9
6	154406.5	169160.5	201431.0
7	492693.5	539819.3	645477.0

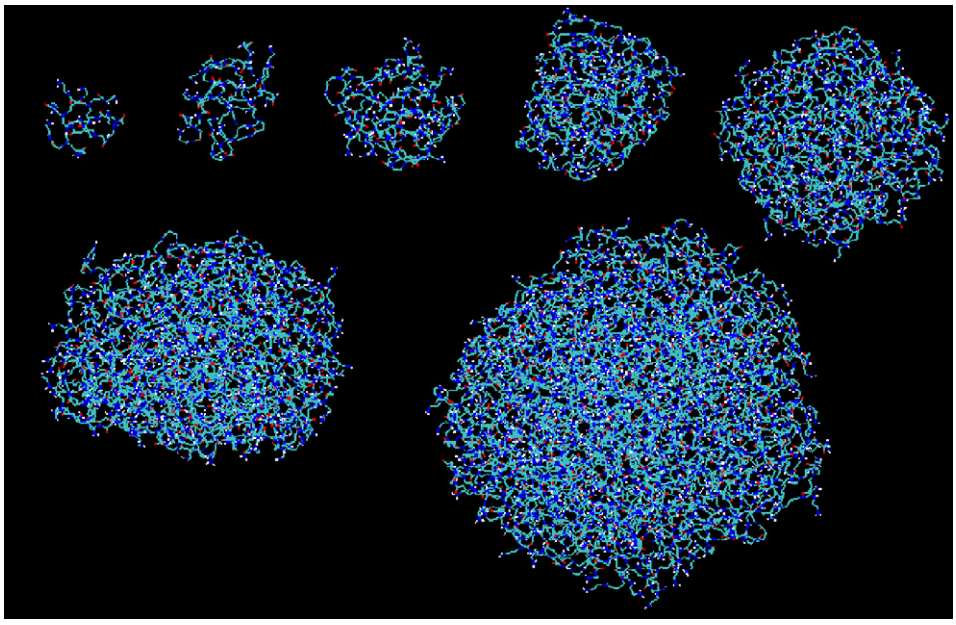

Fig. 3. Typical equilibrated conformations of generation 1 through 7.

spherical structures. The higher generations G5–G7 assume a more globular structure than G1–G4 although the relative shape anisotropy do not decrease monotonically from G1 to G7.

We checked the position of the ethylenediamine core carefully to see if it stays in the center of the spheres. We measure the distance between the centers of mass of the whole dendrimer and of the DEA core. The average distances are 0.15, 0.50, 0.62, 0.65, 0.26, 0.27 and 0.29 nm for G1 to G7, respectively. So it is obvious that the core deviates from the center of the spheres, especially for the low generations. The structures in geometry are not symmetry.

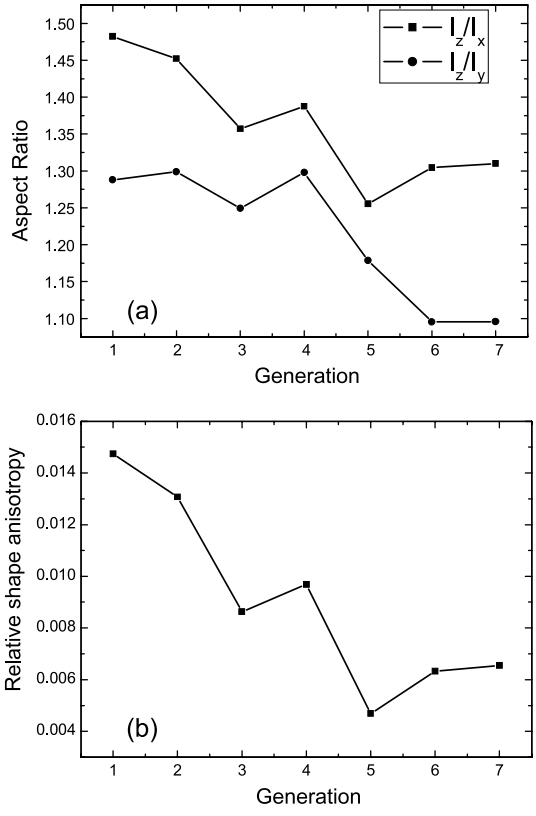

Fig. 4. (a) Moment of inertia based aspect ratios as a function of generation. (b) Relative slope anisotropy as a function of dendrimer generation.

3.3. Monomer density distribution and terminal amine group distribution

3.3.1. Monomer density distribution

The conformation of dendrimer is most conveniently expressed through the average radial monomer density $\rho(r)$, which is calculated from the configurations by counting the number of atoms whose centers are within a spherical shell of radius r and thickness Δr. Hence, the integration over r yields the total number of atoms $N(r) = 4\pi \int_0^{\infty} r^2 \rho(r)\, dr$, where r is the distance from the center of mass of the dendrimers. This number was divided by the volume of the shell to produce $\rho(r)$. We used $\Delta r = 0.1$ nm. Smaller Δr will be too noisy.

The monomer number density as a function of the distance $\rho(r)$ is shown in Fig. 5a. The curves corresponding to seven generations are depicted. In each case, we take the origin as the center of mass. In Fig. 5b each curve is shifted from the previous one by 50 in the vertical axis. In the region near the center of the mass the behaviors of the density are very different. The density of generation 2, 3, 4 and 6 is low; the density of generation 7 is the same as the other part near this region; the density of generation 1 and 5 is high and has a local minimum. We think the value in this region is too noisy to be reliable because the error is big

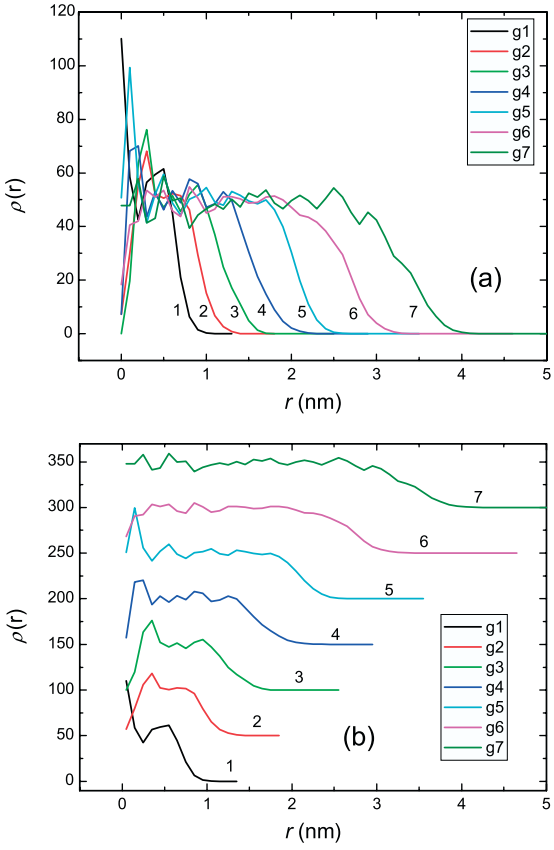

Fig. 5. Radial monomer density of PAMAM, each curve is shifted from the previous one by 50 in the vertical axis in (b).

when the number is divided by the too small volume within the shell near the center of the mass. We changed Δr from 0.1 to 0.4 nm for generation 5 in Fig. 6. We can see that the bigger Δr is, the smoother the curve is. When we use 0.4 nm the density is almost uniform from the center of the mass. In the result of Murat and Grest's work [14] by the coarse-grained model they found very high density in the core region and a local minimum near the core region. In Maiti and Goddard et al.'s work [5] they found that the core

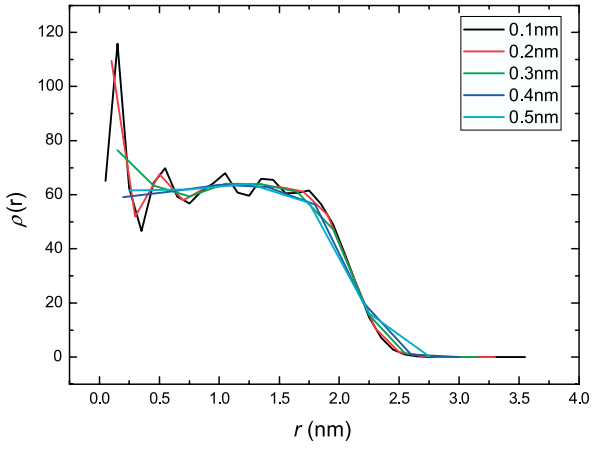

Fig. 6. Radial monomer density of generation 5 by different Δr.

domain is dense for generations up to G7 but that for higher generations it drops dramatically. We suspect their high density results from the too small volume of the shell near the center of the mass too. They do not mention if the position of the initiator core of the dendrimer coincides with the center of the mass in their model. So we are not sure the high-density zone lies in the core region of the dendrimer in their model. In our model the core deviates from the center of mass and the dendrimers here have not perfect symmetrical structures. Thus, the density measured in the region of the center of the mass is not for the core part. Following the zone of the center of the mass there are distinct plateaus from generation 2 to 7. The constant density zone broadens with increasing generation value. The value of the density in this constant density zone is virtually identical for all the generations. The constant density region is followed by a tail zone, where the density decays monotonically toward the exterior of the molecule. In the work by Murat and Grest [14] they found the constant density zone too and found it is the same for different generations while in Maiti and Goddard et al.'s work [5] they found the constant density region but monomer density in this constant density region increases with the generation.

Prosa, Tomalia and Scherrenberg [13] studied PAMAM in dilute methanol (MeOH) solutions by using small-angle X-ray scattering. Their comparisons of experimental particle scattering curves with scattering curves from various model electron density distributions indicate that the dendrimers, especially the larger generations, consist of a relatively monodisperse distribution of constant density spheres. The average density of the dendrimers appears to be roughly independent of generation. The result is the same as what we got by simulation here.

Both the EDA core and the generations (the repeating units attached to the core) are flexible because of the methylene groups. The DEA core consists of the same groups as the generations except the peptide bonds. In the situation that we simulate the vdW interaction play an important role. The similar chemical components between core and generations should have similar interaction and similar structure. So we think it is reasonable for the PAMAM dendrimer to have a uniform density distribution. When the generation number increases the similarity keeps the same, so the density is independent of the generations. These constant density models is very different with the dense-shell model of de Gennes and Hervet [18] and the dense-core model of Lescanec and Muthukumar [19]. From this simulation we suppose that different chemical components should have different structures, even the same dendrimers in different surrounding conditions should have different structures.

3.3.2. Terminal group distribution

The surface activities of the PAMAM dendrimers in solution depend strongly on the location of the terminal groups and their distribution within the molecule. The

density profile for the primary nitrogen atom is calculated to quantify how much the terminal groups are back-folded into the interior portion of the dendrimer. As shown in Fig. 7 the end groups are distributed throughout the dendrimers. For G1 through G4 there is a peak near the radius of gyration of the dendrimer while for G5 through G7 the density is almost uniform and different generations have similar density. In the equilibrated configurations we can find the end groups come close to the core of the molecule. A large number of primary nitrogen atoms crowd into the core especially for the higher generations. So end groups of PAMAM are sufficiently flexible to interpenetrate nearly the whole molecule. The highly flexibility is one of the specific properties of PAMAM dendrimers and makes the compact structure possible.

3.4. Dendrimer and water interface

Since most of the specific application of dendrimers involves interaction with their outer exposed surface, their full characterization is of prime importance. Here we measure the radial density distribution of the solvent water and compare it with the dendrimer density distribution in Fig. 8. The water density is zero in the dendrimer zone, from

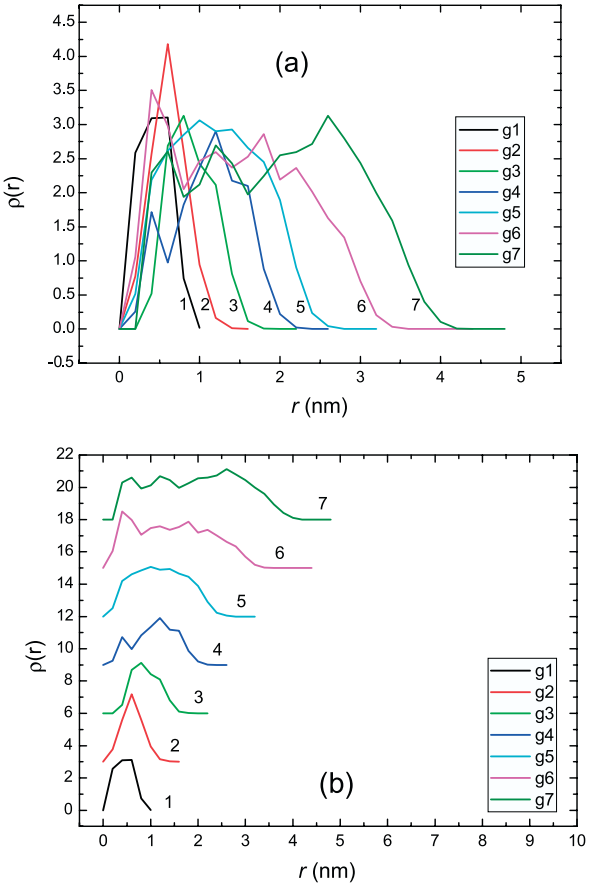

Fig. 7. Radial primary nitrogen density of PAMAM, each curve is shifted from the previous one by 3 in the vertical axis in (b).

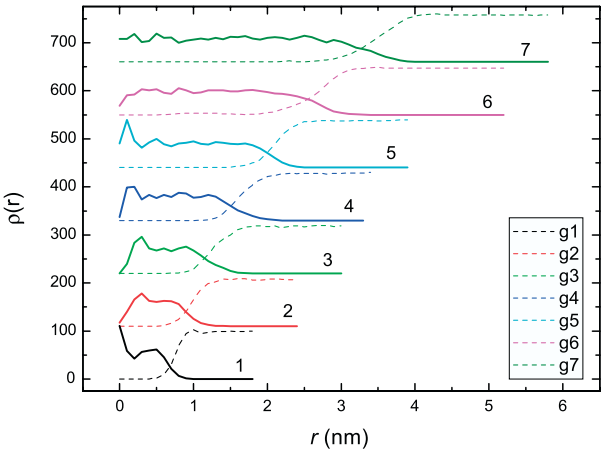

Fig. 8. Radial density for the dendrimer and water, each curve is shifted from the previous one by 110 in the vertical axis.

the region of interface it increases to a constant zone. There are overlaps in the interface, which results from the asphericity of the dendrimers.

The solvent accessible surface is traced out by the probe sphere center as it rolls over the dendrimers. To calculate solvent accessible surface, we have used the double cubic lattice method (DCLM) [20] which is implemented in GROMACS. In Fig. 9 the dependence of the root of solvent accessible surface on the probe radii is plotted. If the probe radii are larger than the largest internal void, the root of solvent accessible surface increases linearly with the probe radius. We fit the points for the bigger radii. The difference between the calculated points and the line in Fig. 9 indicates the presence of internal area of the pores and internal voids in dendrimers. However, when we checked the configuration of the dendrimers water penetration to the dendrimer is not observed. We used water as the probe molecule (radius = 0.14 nm) to get the solvent accessible surface as the function of the generations shown in Fig. 10a. Surface fractal analysis is applied in Fig. 10b. We get the scaling property of solvent accessible surface $\sim R_g^{2.10}$, where the

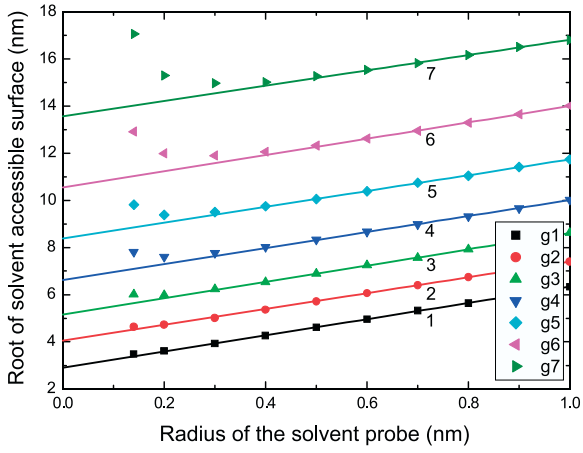

Fig. 9. Root of solvent accessible surface as a function of probe radius.

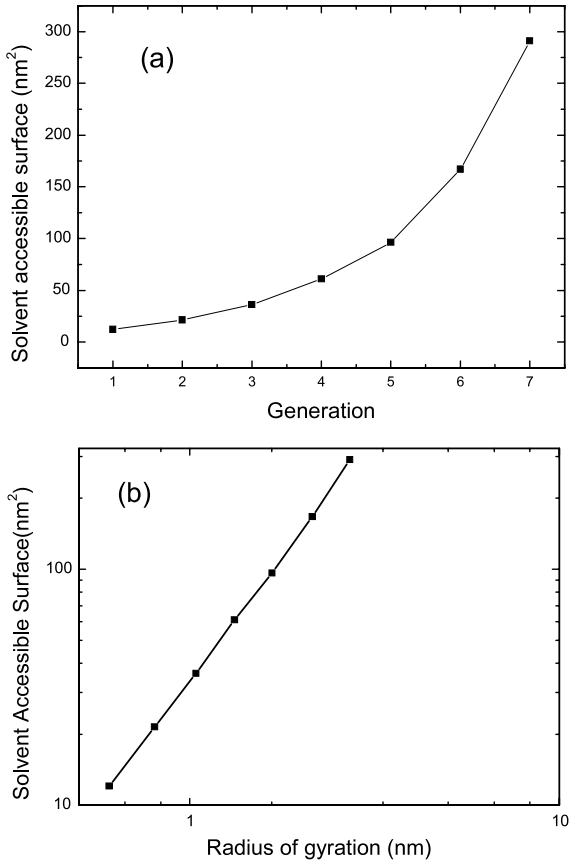

Fig. 10. (a) Solvent accessible surface area as the function of the generation. (b) Relationship between the solvent accessible surface and the radius of gyration of the dendrimers.

exponent is near 2, indicating the surface is smooth and the objects are densely compact. It is in agreement with the scaling property of the number of atoms with the radius of gyration. Thus we think in the condition that we did the simulation, that is, pH over 10 aqueous solution the PAMAM dendrimers are particles with rather sharp boundary. In the interface hydrogen bonds can be found.

3.5. Diffusion

As for the kinetic properties we discuss the mean square displacement (MSD) in addition to the autocorrelation function. As a kind of colloid particles PAMAM has Brownian dynamic behavior. The mean square displacement is a measure of the average distance a molecule travels. From the slope of the mean square displacement curve of the center of mass of the particles versus time, the diffusion constant D can be evaluated using the Einstein relation:

$$D = \lim_{t\to\infty} \frac{1}{2dt} msd(t) = \lim_{t\to\infty} \frac{1}{2dt} \langle |r(t) - r(0)|^2 \rangle$$

where $r(t)$ stands for the position vector of a particle at time t, and the brackets denote an ensemble average. The number of dimensions is given by the factor d: $d=1$ for linear, $d=2$ for lateral, and $d=3$ for bulk diffusion. Fig. 11 shows the MSD of the dendrimers. Within 500 ps the dendrimer molecules diffuse on a nanometer scale. The diffusion constant is presented in Fig. 12 by least squares fitting a straight line of MSD. As shown in Fig. 12 the generation value of a dendrimer heavily influences its dynamic behavior. The diffusion constant decreases from 3.51×10^{-8} cm^2/s for G1 to 3.9305×10^{-9} cm^2/s for G7 monotonically. The results indicate a slowing of molecular motions as molecular size increases, which is in agreement with ^{13}C NMR relaxation measurements [21]. The diffusion constant of the solvent water is 4.329×10^{-5} cm^2/s, a faster diffusion compared to the dendrimer molecules.

4. Conclusions

We studied the atomistic force field based MD study of PAMAM dendrimers G1 through G7 in explicit water solution. The autocorrelation function of the squared radius of gyration is measured to confirm the simulation time is long enough for sampling. No amines are assumed to be protonated so the simulation condition is designed to represent the dilute alkali solution. All the generations are spherical in shape, while the higher generations show edges or slightly polyhedral shape. The DEA core deviates from the center of the mass. The density profile indicates that the dendrimers are constant density spheres and the densities are independent of generation in this aqueous solution. The scaling properties of the radius of gyration with the numbers of atoms and solvent accessible surface with radius of gyration indicate the PAMAM dendrimers are densely compact structures. The compact structures result from the highly flexibility confirmed by the terminal group distribution. As a kind of colloid particle the diffusion behavior was studied too. The bigger the dendrimers the more slowly the particle moves. From the comparison with other models such as dense-core or dense-shell model we think the chemical components and the situation decide the structure

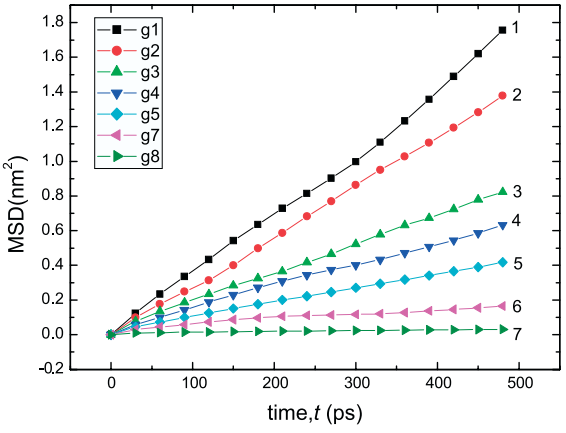

Fig. 11. Mean square displacement of dendrimers in this simulation.

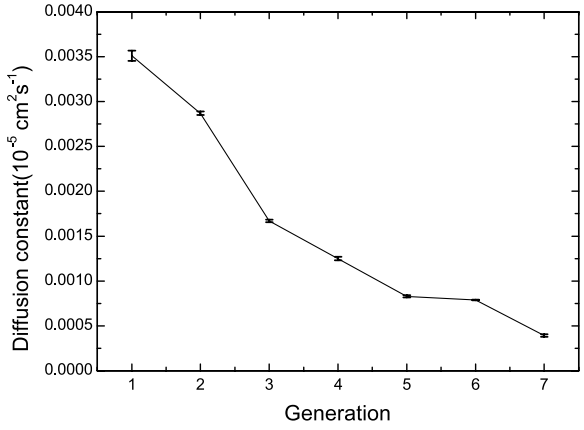

Fig. 12. Diffusion constant as the function of the generation.

of the dendrimer. Not all the dendrimers have the same spatial distribution style.

In the real experiment the effect of protonation plays important role. In the future we should perform the simulation about the protonized state of the dendrimers, where the electrostatic interaction will be considered more carefully.

Acknowledgements

The authors acknowledge the financial support from National Natural Science Foundation of China (including 20490220), 863 Project and 973 (2004CB720606) Project.

References

[1] Matthias B, Christos NL. Angew Chem Int Ed 2004;43:2998–3020.
[2] Tomalia DA, Baker H, Dewald J, Hall M, Kallos G, Martin S, Roeck J, Ryder J, Smith J. Polym J 1985;17:117–32.
[3] Fréchet JMJ, Tomalia DA. Editor dendrimers and other dendritic polymers. New York: Wiley; 2001.
[4] Tomalia DA, Dvornic PR. Dendritic polymers, divergent synthesis (Starburst polyamidoamine dendrimers). In: Salamone JC, editor. Polymeric materials encyclopedia. Boca Raton: CRC Press; 1996. p. 1814–30.
[5] Maiti PK, Cagın T, Wang GF, Goddard WA. Macromolecules 2004; 37:6236–54.
[6] Lee I, Athey BD, Wetzel AW, Meixner W, Baker JR. Macromolecules 2002;35:4510–20.
[7] Spoel D, Lindahl E, Hess B, Buuren AR, Apol E, Meulenhoff PJ, Tieleman DP, Sijbers ALTM, Feenstra KA, Drunen R, Berendsen HJC. Gromacs User Manual version 3.2 2004.
[8] Lindahl E, Hess B, Spoel D. J Mol Mod 2001;7:306–17.
[9] Berendsen HJC, Postma JPM, Gunsteren WF, Hermans J. Interaction models for water in relation to protein hydration. In: Pullman B, editor. Intermolecular forces. Dordrecht: Reidel; 1981. p. 331–42.
[10] Berendsen HJC, Postma JPM, Gunsteren WF, DiNola A, Haak JR. J Chem Phys 1984;81:3684–90.
[11] Hess B, Bekker H, Berendsen HJC, Fraaije JGEM. J Comput Chem 1997;18:1463–72.
[12] Miyamoto S, Kollman PA. J Compos Chem 1992;13:952–62.
[13] Prosa TJ, Bauer BJ, Amis EJ, Tomalia DA, Scherrenberg RJ. Polym Sci, Part B: Polym. Phys. 1997;35:2913–24.
[14] Murat M, Grest GS. Macromolecules 1996;29:1278–85.
[15] Humphrey W, Dalke A, Schulten K. J Mol Graph 1996;14:33–8.
[16] Jackson CL, Chanzy HD, Booy FP, Drake BJ, Tomalia DA, Bauer BJ, Amis EJ. Macromolecules 1998;31:6259–65.
[17] Theodorou DN, Suter UW. Macromolecules 1985;18:1206–14.
[18] de Gennes PG, Hervet H. J Phys Lett 1983;44:351–60.
[19] Lescanec RL, Muthukumar M. Macromolecules 1990;23:2280–8.
[20] Frank E, Philip L, Patrick A, Chris S, Michael S. J Compos Chem 1995;16:273–84.
[21] Meltzer AD, Tirrell DA, Jones AA, Inglefield PT, Hedstrand DM, Tomalia DA. Macromolecules 1992;25:4541–8.